applied sciences

MDPI

Article

Physicochemical Characterization of a Cellulosic Film Modified with Two Room-Temperature Ionic Liquids

Maria del Valle Martinez de Yuso [1], Ana Laura Cuevas [2] and Juana Benavente [3,*]

[1] Laboratorio de Espectroscopía de Fotoelectrones de Rayos X (SCAI), Universidad de Málaga, E-29071 Málaga, Spain
[2] Unidad de Nanotecnología, Centro de Supercomputación y Bioinnovación, Servicios Centrales de Investigación, Universidad de Málaga, E-29071 Málaga, Spain
[3] Departamento de Física Aplicada I, Facultad de Ciencias, Universidad de Málaga, E-29071 Málaga, Spain
* Correspondence: j_benavente@uma.es

Abstract: Changes in the physicochemical characteristics of a regenerated cellulose (RC) film due to a surface modification with room-temperature ionic liquids (ILs) are determined. Two ILs (1-butyl-3-metylimidazolium hexafluorophosphate and tricaprylmethylammonium chloride) were selected, and film surface modification was performed by a dip-coating process (1 h) in the corresponding IL. The surface characterization of the RC/IL films was carried out by XPS at various take-off angles (from 15° to 75°), while the modification of mechanical properties was established by tensile analysis, obtaining a significant increase for the Young modulus of both RC/IL films when compared with the RC-support. Optical characteristics of the RC/IL films were determined by transmittance and reflectance measurements for wavelengths covering visible and near-infrared regions, while impedance spectroscopy (IS) measurements allow us to estimate the electrical changes in the RC/IL films. These results show the high transmittance of both RC/IL films (>90%) with slight differences depending on the IL in both optical regions, while the IS data analysis indicated a conductivity reduction and dielectric constant increase in the dielectric constant for both eco-friendly RC/IL films.

Keywords: film modification; ionic liquids; XPS; mechanical effect; optical and electrical changes

Citation: Yuso, M.d.V.M.d.; Cuevas, A.L.; Benavente, J. Physicochemical Characterization of a Cellulosic Film Modified with Two Room-Temperature Ionic Liquids. *Appl. Sci.* **2022**, *12*, 10290. https://doi.org/10.3390/app122010290

Academic Editors: Ivo Stachiv, Sneha Samal and David Vokoun

Received: 21 September 2022
Accepted: 10 October 2022
Published: 13 October 2022

1. Introduction

Room-temperature ionic liquids (RTILs), or more simply, ionic liquids (ILs), have attracted a great deal of attention from the mid-1970s as environmentally friendly alternatives to volatile organic compounds. As it is well known, ILs are molten salts with a very low vapor pressure composed of an organic cation and an organic/inorganic anion, which remain in the liquid state for temperatures below 100 °C. Moreover, other significant properties of ILs such as their high solubility, thermal stability, water sensitivity and eco-friendly character, as well as their elevated ionic mobility and viscosity, are nowadays characteristics of great interest in diverse research and industrial areas [1]. In fact, the particular properties of ILs allow for their use in a large number of different applications, such as solvents for organic reactions and catalysis, electrodeposition, extraction, energy, membranes for separation processes, electrochemical devices (capacitors, fuel cells, batteries or solar cells) or optical sensors [2–12]. Imidazolium-based ILs (1-methyl-3-butylimidazolium tetrafluoroborate, 1-methyl-3-butylimidazolium bromide, 1-allyl-3-methylimidazolium chloride, 1-ethyl-3-methylimidazolium tetrafluoroborate, 1-methyl-3-butylimidazolium hexafluorophosphate, . . .) are commonly used in such applications, but trioctylmethylammonium chloride (or AliquatCl) and its derivatives (AliquatNO_3 or AliquatSCN), n-dodecyltriethylammonium chloride (or DTACl) and many others ILs are also usually considered [13–15]. In fact, a significant aspect of ILs is the possibility of tailoring their physicochemical properties via the selection of the cation/anion, which enables researchers to obtain ILs with the most adequate characteristics for a specific

application. Additionally, since the liquid state of ILs is not associated with solvent presence, they are considered green products, and different hybrid IL/biopolymer materials are being studied for biomedical applications [16].

In this context, the modification of polymeric membranes by different ILs for applications in many separation processes (fuel and microbial cells, CO_2 separation, ...) has already been reported [17–21]. In particular, the surface modification/incorporation of various ILs in Nafion membranes by immersion in solutions with different percentages of IL via the proton/cation exchange process has been performed to improve the thermal stability of membranes, which might favor their possible application as polymer electrolyte membranes at high temperatures or for methanol and gas crossover reduction in the case of direct methanol fuel cells [22–25]. Moreover, ILs are also used in the fabrication of polymer inclusion membranes (PIMs), with applications in the separation of different kinds of compounds (anions, metallic species or small organic molecules), as a way to improve their mechanical stability when cellulose triacetate or polyvinyl chloride is used as the polymeric matrix [26–30]. Another polymeric but biocompatible material widely used for membranes or thin films manufacturing is regenerated cellulose (RC), and different cellulose–ILs hybrid materials for drug delivery, biosensing or tissue engineering applications have already been reported [16,31]. On the other hand, the modification of regenerated cellulose (RC) films with lipids or ILs layers and/or the incorporation of different nano-structures (nanoparticles, dendrimers or different kinds of quantum dots) by simple dip coating in aqueous solutions of the modifying agents (without any chemical reaction) has also been reported, with the simplicity of this modification process being associated with the high hydrophilic character and swelling degree of the RC-support [32–36]. In this context, it should be indicated that the high transparency of cellulosic films is a characteristic of significant interest nowadays due to its importance for applications in optical devices [37,38], but their biocompatibility is another factor of great significance [16].

In this work, we analyze optical and electrical changes in a RC film modified by the incorporation of two ILs ($BMIMPF_6$ or AliquatCl) with different structures and characteristics (aromatic ring/aliphatic chain length, molecular weight or viscosity) via the dip-coating process. Changes in the surfaces of both modified films (RC/$BMIMPF_6$ and RC/AliquatCl films) were determined by XPS analysis, while the modification of elastic properties was established from the stress–strain curves. Optical changes associated with the presence of the ILs on the surfaces of the RC-support were obtained by light transmission and reflection measurements for visible (400–800 nm) and near-infrared (800–2000 nm) regions, while impedance spectroscopy measurements were performed to determine modifications in the electrical characteristic parameters (conductivity and dielectric constant) of the RC/Il films. These results showed that IL inclusion by a simple dip-coating process slightly changed the transmission/reflexion of the RC-support, affecting values of conductivity and dielectric constant in a certain percentage, but significantly increasing the elastic modulus of both RC/ILs films. Moreover, the green and/or biocompatible character of the attained RC/IL films can be a factor of interest.

2. Materials and Methods

Two ILs, tricaprylmethylammonium chloride ($C_{25}H_{55}N^+Cl^-$ or AliquatCl) and 1-butyl-3-metylimidazolium hexafluorophosphate ($C_8H_{15}N_2{}^+PF_6{}^-$ or $BMIMPF_6$), both from Sigma-Aldrich (St. Louis, MO, USA), were selected for cellulosic film modification and were used without further purification. AliquatCl is a quaternary ammonium salt (a 2:1 mixture of methyl trioctyl- and methyl tridecylammonium chloride), while $BMIMPF_6$ is an imidazole-based IL exhibiting an aromatic ring and shorted aliphatic chain, as can be seen in the Supplementary Information (Figure S1) where the structure of both ILs and cellulose is indicated. The molecular mass, density and viscosity of the ILs were: 284.2 g/mol, 1380 kg/m^3 and 267 mPa.s for $BMIMPF_6$, but 432 g/mol, 886 kg/m^3 and 1500 mPa.s (at 25 °C) for AliquatCl [39].

A highly swelling and transparent film of regenerated cellulose (RC) from Cellophane Española S.A. (Burgos, Spain) was selected for ILs modification via the dip-coating process, and samples of the RC film were submerged for 1 h in an open glass flask containing the corresponding IL. These samples will hereafter be called the RC/AliquatCl and RC/BMIMPF$_6$ films.

A chemical surface characterization of the films was performed by a Physical Electronics spectrometer (PHI 5700) with X-ray Mg K$_\alpha$ radiation (300 W, 15 kV, 1253.6 eV) as the excitation source. High-resolution spectra were recorded by a concentric hemispherical analyzer operating in the constant pass energy mode at 29.35 eV, using a 720 µm diameter analysis area. Although the optimum equipment take-off angle was 45°, angle resolved XPS measurements (ARXPS) were performed for an in-depth surface analysis (without sample damage) by using five different take-off angles: ϕ = 15°, 30°, 45°, 60° and 75°, taking into account the relation between the escape depth (d) and the photoelectron mean free path (λ) [40,41], $d \leq 3\,\lambda \sin\phi$, which enabled us to obtain chemical information from depths ranging between 2.5 nm (ϕ = 15°) and 9.3 nm (ϕ = 75°), assuming the mean free path (λ) in polymers for the C 1*s* excited photoelectrons was 3.2 nm [42]. Samples were kept overnight at a high vacuum (preparation chamber) and were then transferred to the analysis chamber for testing, and each spectral region was scanned several times until a good signal-to-noise ratio was observed. Binding energies were determined with respect to the position of the adventitious C 1*s* peak at 285.0 eV (accurate ±0.1 eV), and the residual pressure in the analysis chamber during the data acquisition was maintained below 5×10^{-7} Pa. The PHI ACCESS ESCA-V6.0 F software package was used for acquisition and data analysis. To accurately determine the binding energy (BE) of the different element core levels, recorded spectra were fitted using Gauss–Lorentz curves as was already described in detail [43]. Atomic concentration percentages (A.C. %) of the characteristic elements found on the surface of the analyzed samples were determined taking into account the corresponding area sensitivity factor for each measured spectral region [44].

Films elastic measurements were performed at laboratory atmospheric conditions with a force digital gauge (Mark-T, ES20 model) connected to a computer, with a maximum tension of 100 N, length accuracy of ±0.01 mm and a strength rate of 0.167 mm/s.

Light transmittance and reflection measurements were carried out with a Varian Cary 5000 spectrophotometer (Agilent Technologies, Santa Clara, CA, USA) provided with an integrating sphere of Spectralon for wavelengths ranging between 200 nm and 2000 nm, which allowed us to obtain information on visible and near-infrared (nir) regions.

Impedance spectroscopy (IS) is an alternating current (a.c.) technique commonly used for the electrical characterization of homogeneous materials or homogeneous layered samples. SE measurements for the RC/IL films were carried out at room atmospheric conditions using a cell formed by two Pt electrodes embedded in a Teflon support and closed with four screws (system: Pt-electrode//film//Pt-electrode), with the electrodes connected to a Frequency Response Analyzer (FRA, Solartron 1260, Farnborough, England). The impedance (Z) is a complex number, with real (Z_{real}) and imaginary (Z_{img}) parts, that is, $Z = Z_{real} + i\,Z_{img}$ (where i denotes the imaginary unity), which are related to both the transport of charge across the membrane and charge storage by means of the electrical resistance (R) and capacitance (C). The IS characterization technique allows for the estimation of R and C by analyzing the Nyquist plot ($-Z_{img}$ vs. Z_{real}), using equivalent circuits as models [45,46]. IS measurements were carried out for frequency (f) ranging from 1 Hz to 10^7 Hz (100 data points) at a maximum voltage of 0.01 V, and characteristic electrical parameters for the studied samples were determined using the data analysis program ZView 2 (Scribner, Southern Pines, NC, USA).

3. Results and Discussion

3.1. Chemical Surface Characterization of the RC/IL Films

Chemical surface characterization of the RC/IL films was performed via the XPS technique, which gives information of the elements present on the surface of a given

sample by analyzing the high-resolution spectra. XPS survey spectra at a take-off angle of 45° for both RC/IL samples are given as Supplementary Information (Figure S2), where the photoemission lines corresponding to the characteristic ILs elements are indicated (C, N, F, P for the RC/$BMIMPF_6$ film or C, N, Cl for the RC/Aliquat film), but the presence of two other non-characteristic elements, oxygen and silicon, associated with the cellulosic support (characteristic or impurities elements) are also indicated, and this point will be discussed later.

The atomic concentration percentage (A.C. %) of the ILs characteristic elements detected on the surface of the RC/IL films were obtained by the corresponding curve area, as shown in Figure 1 for the core level spectra of the different elements. As can be seen in Figure 1a, the C 1*s* signals obtained for the RC/$BMIMPF_6$ film shows: (i) a clear peak at a binding energy (B.E.) of 285.0 eV (C_1), which corresponds to aliphatic carbon, additives or pollution (-CH-, -C-C-, β-C) [47] and represents 55.9% of the total carbon contribution, (ii) a certain plateau (C_2, from 286.1 eV to 286.6 eV) associated with the imidazolium group, C=N and C-N bonds (33.2% of the total area) [41] although it might also include C-O bonds from the support, (iii) a small shoulder (C_3, at around 289.0 eV and 10.9% of area) associated with the O=C-O, CO_3 bonds from the support [47], as can be observed in Figure 1b, where a comparison of the normalized C 1*s* spectra obtained for the $BMIMPF_6$ IL, the RC/$BMIMPF_6$ film and the RC-support is shown. The C 1*s* spectra corresponding to the RC/AliquatCl film also showed a significant peak at the B.E. of 285.0 eV (72.6% of the total area), higher than that exhibited by the RC/$BMIMPF_6$ film in agreement with its higher aliphatic chain, plus two small shoulders, at 286.2 eV (21.7% of area) and at 287.8 eV (5.6% of carbon area), associated with C-O and O-C-O bonds, respectively, both from the RC-support.

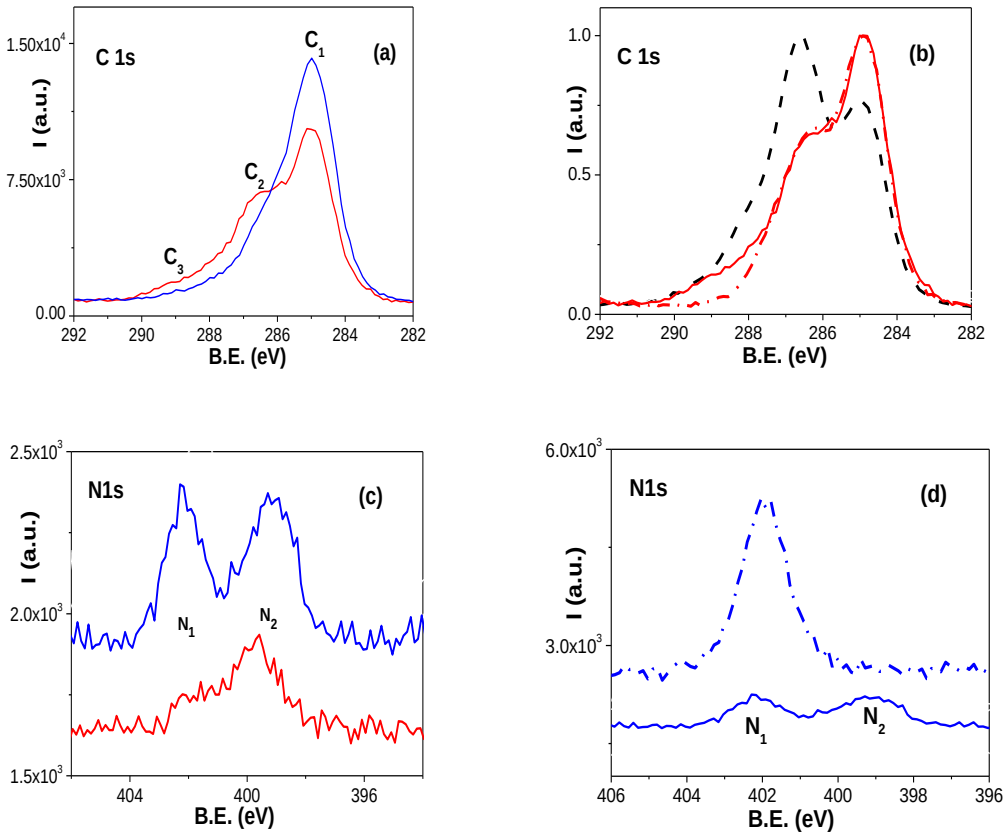

Figure 1. Core level spectra signals for: (**a**) C 1*s* for RC/AliquatCl film (blue solid line) and RC/$BMIMPF_6$ film (red solid line); (**b**) comparison of normalized C 1*s* signal for the RC/$BMIMPF_6$ film (red solid line), RC-support (black dashed line) and $BMIMPF_6$ IL (red dashed–dot line); (**c**) N 1*s* (blue solid line) for RC/AliquatCl film and red solid line for RC/$BMIMPF_6$ film; (**d**) comparison of N 1*s* signal for the IL AliquatCl (blue dashed–dot line) and the RC/Aliquat (blue solid line).

The N 1*s* core level spectra obtained for both RC/IL films is shown in Figure 1c, where two peaks, N_1 and N_2, at around 402.2 eV and 399.4 eV can be observed; the comparison of the N 1*s* signal obtained for the RC/AliquatCl film and the AliquatCl IL presented in Figure 1d clearly shows the correspondence of the peak at 402.2 eV (N_1) with that exhibited by the IL, while the N_2 peak is associated with support impurities that could depend on the sample water content, as it was obtained for polymeric inclusion membranes fabricated with 60% of AliquatCl and 40% of cellulose triacetate [14], and it is provided as Supplementary Information (Figure S3a). In the case of the RC/BMIMPF$_6$ film, the peaks are related to the C-N link and protonated nitrogen, respectively; a comparison of nitrogen normalized spectra for the RC/BMIMPF$_6$ and the BMIMPF$_6$ IL is also given as Supplementary Information (Figure S3b).

Figure 2a,b show the fluorine and phosphorous core level signals for the RC/BMIMPF$_6$ film, while the chlorine spectra for the RC/AliquatCl film is shown in Figure 2c, where that obtained for the AliquatCl IL is also indicated; the oxygen core level signal for both RC/IL films and the RC-support is drawn in Figure 2d, showing the three samples a symmetrical peak at the same B.E., which confirms the adscription to the RC-support of the oxygen content determined for both RC/IL films.

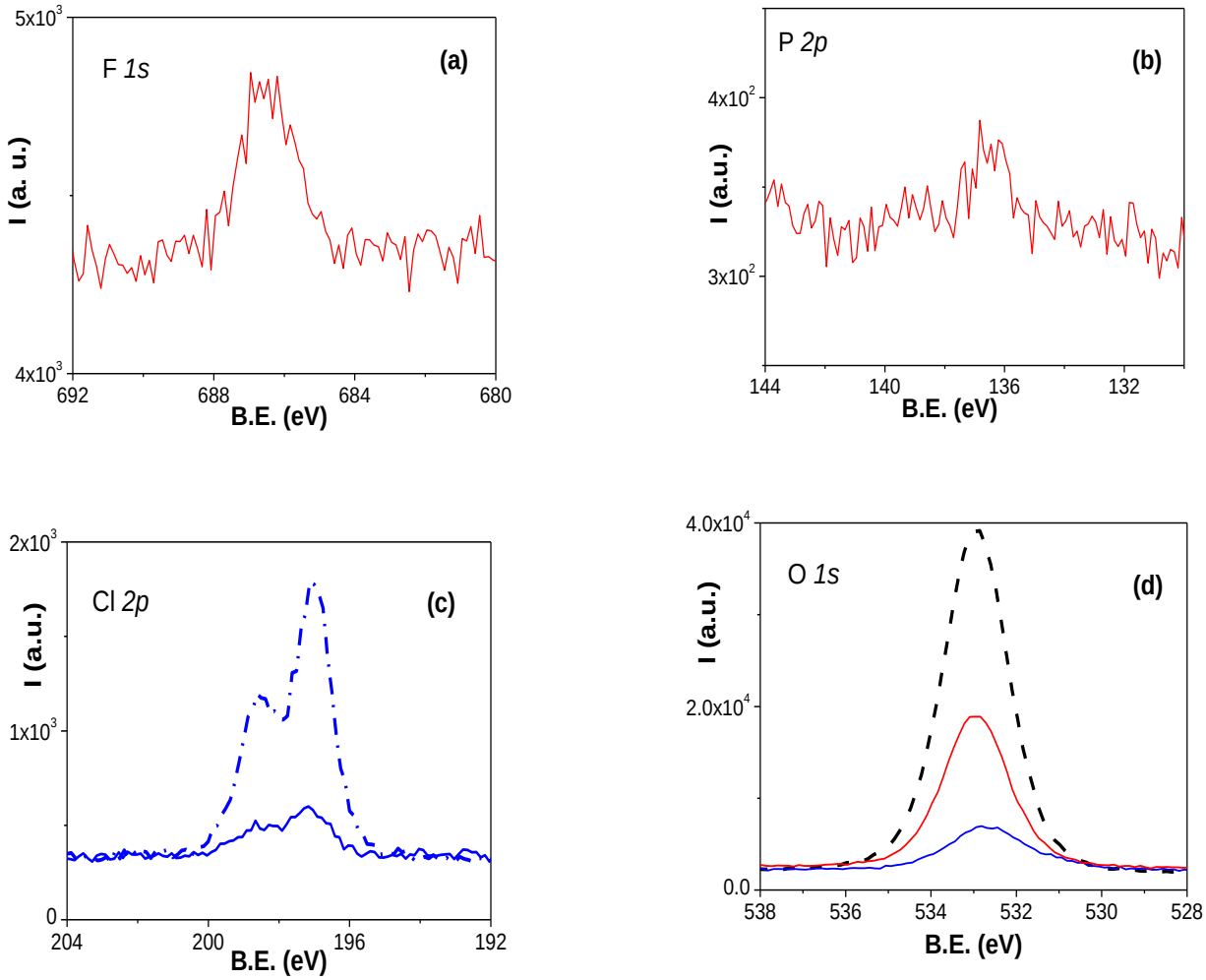

Figure 2. (**a**) Fluorine and (**b**) phosphorous core level signals for the RC/BMIMPF$_6$ film. (**c**) Comparison of chlorine signals for the RC/AliquatCl film (blue solid line) and the AliquatCl IL (blue dashed–dot line. (**d**) Oxygen core level signals for the RC/BMIMPF$_6$ film (red solid line), the RC/AliquatCl film (blue solid line) and the RC-support (black dashed line).

Table 1 shows the A.C. % of the different elements founded on the surfaces of the studied RC/IL films and, for comparison reasons, the A.C. % of the chemical elements

determined for the AliquatCl IL and the $BMIMPF_6$ ILs as well as for the RC-support are given as Supplementary Information in Table S1. On the other hand, as was indicated above, two non-characteristic ILs elements such as oxygen and silicon, associated with the RC-support, were also detected on the surface of the RC/IL samples, which is an indication of support surface partial coverage. It should be pointed out that organic compounds with silicon are sometimes purposefully added to polymeric films to improve its plasticity (or an impurity from the monomers purifying columns) [40].

Table 1. Concentration atomic percentages determined at 45° take-off angle for the different elements observed on the surfaces of the RC/AliquatCl and the RC/$BMIMPF_6$ films.

RC/IL Film	C (%)	N (%)	F (%)	P (%)	Cl (%)	O (%)	Si (%)
RC/AliquatCl	83.2	2.7	—	—	0.6	12.6	0.3
RC/$BMIMPF_6$	68.4	1.4	5.1	1.0	—	21. 21.5	1.4

The analysis of the ARXPS spectra allows us to obtain in-deep chemical information of both RC/IL films, and Figure 3 shows the variation with the take-off angle of the atomic concentration % of the elements detected on each RC/IL film; for comparison reasons, the A.C. % of oxygen and silicon obtained for the RC support are also included in Figure 3d,e. These results seem to indicate more homogeneous coverage for the RC/AliquatCl film, taking into account the constancy of the carbon percentage (84 ± 1%) for depths ranging between 2.3 nm and 9.5 nm (see Figure 4a), as well as the lower percentages for oxygen and silicon (support elements) exhibited by this film.

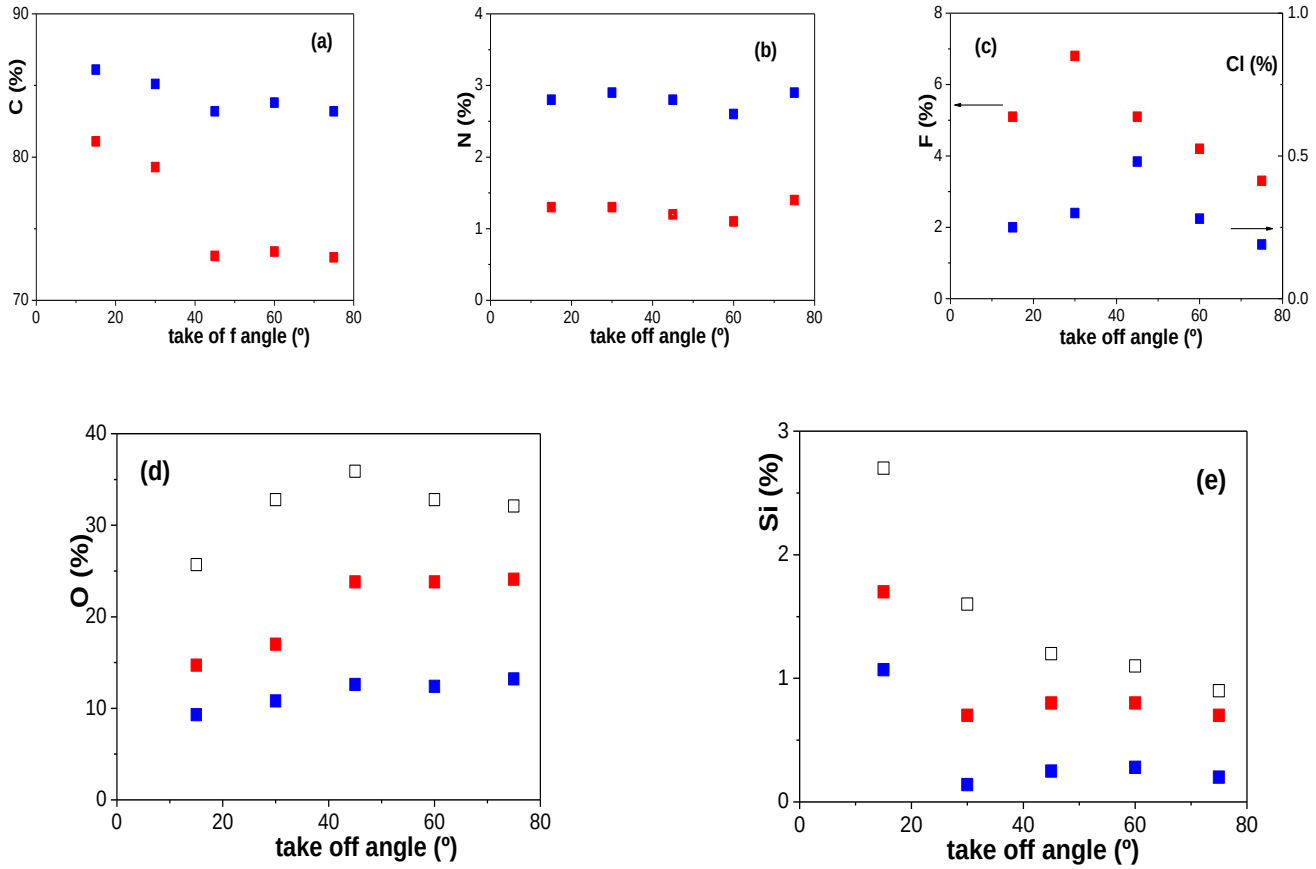

Figure 3. Variation with the take-off angle of A.C. % for: (**a**) carbon; (**b**) nitrogen; (**c**) fluorine or chlorine; (**d**) oxygen; and (**e**) silicon. RC/AliquatCl (blue solid points), RC/$BMIMPF_6$ film (red solid points). Black open points in (**d**,**e**) correspond to the RC support.

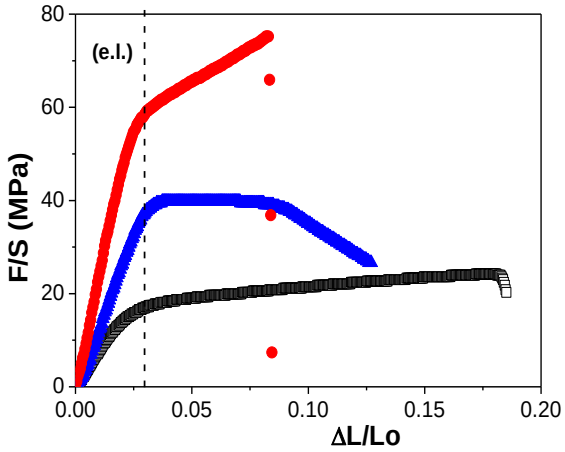

Figure 4. Normal tensile stress versus strain for the RC/BMIMPF$_6$ film (●), the RC/AliquatCl film (▼) and the RC-support film (□).

3.2. Physicochemical Characterization of the RC/IL Films

Changes in the elastic characteristics of the RC support film as a result of the IL modification was expected, taking into account the results previously obtained using other modifying agents (lipid layer coverage, dendrimer inclusion/coating, silver or lipid nanoparticles inclusion, . . . [34,35]); Figure 4 shows the normal tensile stress (F/S) versus strain (ΔL/Lo) curves obtained for both RC/IL films and the RC support, where significant differences in the elastic characteristics of the films can be observed. Although the three samples exhibited a rather similar value for the elastic limit (e.l.~0.03), the curves were clearly different: the strain–stress curve shown by the RC support was similar to that reported by regenerated fibers (viscose or cellulose acetate) and different RC membranes [48,49], with a first part associated with an elastic behavior plus a second and long plastic region, while the RC/IL films showed a higher slope and shorted elongation at break. Since the plastic behavior of RC films can be an impediment for some applications (compaction under pressure), the mechanical properties of cellulose fibers and polymer films can be improved by using silane compounds or other materials [50,51]. In this context, it might be of interest to indicate the significant effect of water content on the elastic behavior of the RC-support, associated with its high hydrophilic character [52], as can be observed in the stress–strain curves obtained for the dry and wet samples of the RC film presented in the Supplementary Information (Figure S3); since elastic measurements were performed at atmospheric conditions, the presence of the ILs might cause a reduction in the water content of the RC/IL films. The elastic (or Young) modulus was determined from the slope of the initial linear dependent part, and the following values were determined: Y(RC/BMIMPF$_6$) = 3.34 GPa and Y(RC/AliquatCl) = 1.52 GPa, which are in the order of values determined for RC films containing ILs [53]; these results indicate an increase of around 372% and 95%, respectively, with respect to the value determined for the RC-support film.

Light transmission and reflexion are non-destructive measurements which provide information of interest on optical characteristics of thin films or layers deposited on a solid matrix [54–56]. Figure 5 shows the transmittance spectra for the two RC/IL films studied, showing high transmittance values (>91%), but slight differences depending on the IL can also be observed in both the visible (400–800 nm, between the two vertical dashed black lines) and the near-infrared (nir) regions, with the light transmittance % being slightly lower for the RC/BMIMBF$_6$ film than for the RC/AliquatCl one, as can be observed in Figure 5a,b. The surface coverage of the RC-support by both ILs seemed to reduce the oscillation in the wavelength interval 1600–2000 nm, moving the RC peak at 1927 nm to 1937 nm and shielding the peak at 1975 nm.

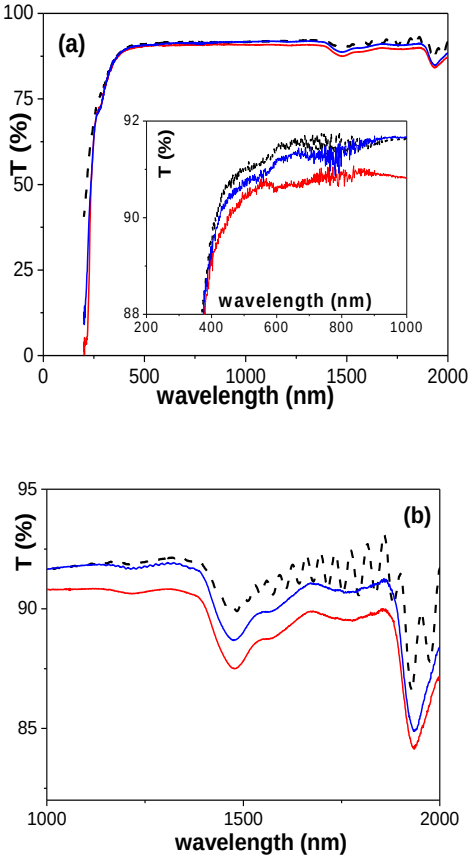

Figure 5. Light transmission as a function of wavelength: (**a**) for the whole range studied; (**b**) for the near-infrared region, for the RC/BMIMPF$_6$ film (red solid line), the RC/AliquatCl film (blue solid line) and the RC-support (black dashed line).

The wavelength dependence of the light reflexion percentage for both RC/IL films and the RC-support is shown in Figure 6, where slight differences in reflexion % in the nir region (14% reduction for the RC/BMIMPF$_6$ film and 6% for the RC/AliquatCl film with respect to the RC-support at 1400 nm) can be observed, but practically similar reflexion percentage values were obtained in the visible region. Consequently, the inclusion of the ILs does not seem to cause changes in the transmission/reflection/absorption characteristics of the RC-support.

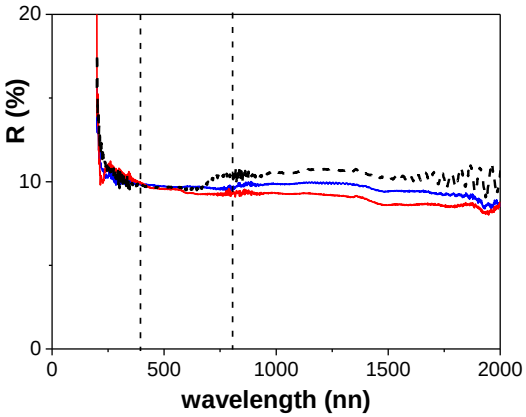

Figure 6. Light reflection as a function of wavelength for the RC/BMIMPF$_6$ film (red solid line), the RC/AliquatCl film (blue solid line) and the RC-support (black dashed line). Visible region: between the two vertical dashed black lines.

Impedance spectroscopy (IS) is another non-destructive technique commonly used for the electrical characterization of materials. IS gives quantitative and qualitative information on systems associated with both bulk and surface (more exactly, the electrode/sample interface) by means of the impedance plots and using equivalent circuits as models [57,58]. Electrical parameters (resistance, R, and capacitance, C) can be determined by analyzing the Nyquist plot (Z_{real} versus $-Z_{img}$), with Z_{real} and Z_{img} being related to the electrical resistance and capacitance by the following expressions [45]:

$$Z_{real} = (R/[1 + (\omega RC)^2]) \quad (1)$$

$$Z_{img} = -(\omega R^2 C/[1 + (\omega RC)^2]) \quad (2)$$

where ω represents the angular frequency ($\omega = 2\pi f$). For homogeneous systems, the Nyquist plot consists of a semi-circle (a unique relaxation time), which corresponds to a parallel association of resistance and a capacitance (RC circuit) with intercepts on the Z_{real} axis at R_∞ ($\omega \to \infty$) and R_0 ($\omega \to 0$), with $R = 0.5(R_0 - R_\infty)$ being the electrical resistance of the system, while the maximum of the semi-circle occurs at a frequency such that $\omega RC = 1$ [45,46]. However, for non-homogeneous systems (two or more relaxation times [40]), depressed semi-circles such as those shown in Figure 7a are commonly obtained, and the equivalent circuit consists of a parallel association of resistance and a non-ideal capacitor (or a constant phase element (CPE)), with the impedance of this latter being expressed by [45]: $Q(\omega) = Y_o(j\omega)^{-n}$, where Y_o represents the admittance (inverse of impedance) while n is an experimental parameter ($0 \leq n \leq 1$), and the equivalent capacitance (C^{eq}) is determined by: $C^{eq} = ([R.Y_o]^{1/n})/R$ [45].

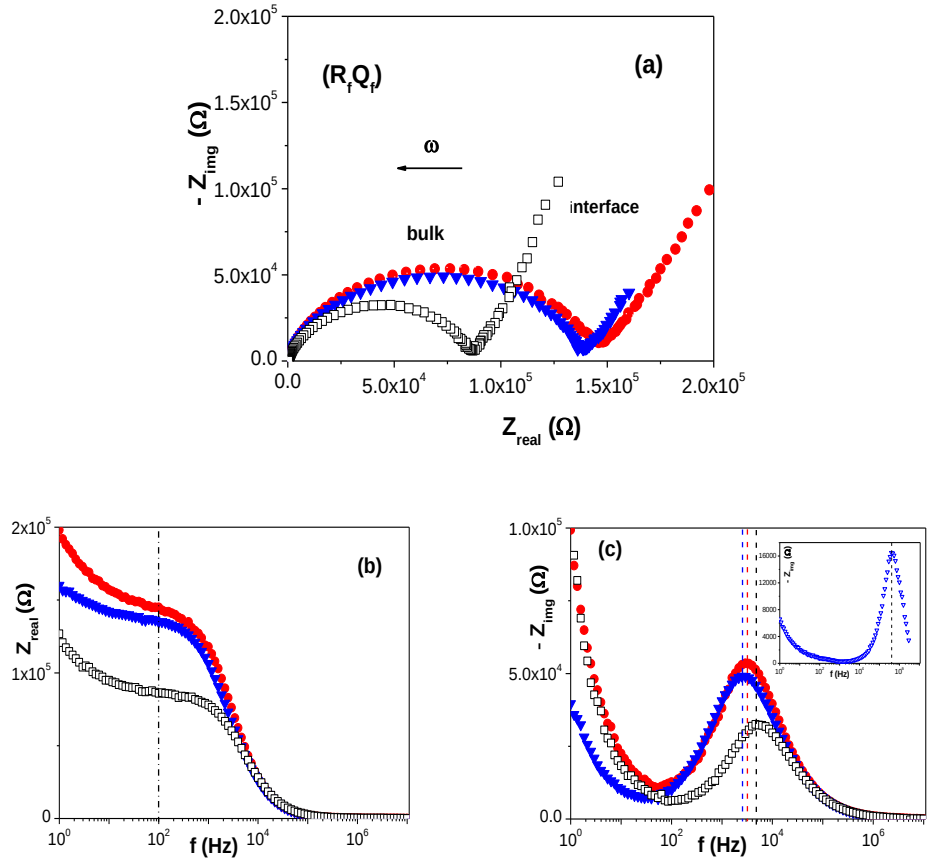

Figure 7. Impedance diagrams for the RC/$BMIMPF_6$ film (•), the RC/AliquatCl film (▼) and the RC support (□). (**a**) Nyquist plot ($-Z_{img}$ vs. Z_{real}); (**b**) and (**c**) Bode plots (Z_{real} vs. frequency) and ($-Z_{img}$ vs. frequency), respectively. Insert in (**b**) and (**c**): Bode plots for the AlqCl IL (▽).

As can be observed in Figure 7a, the Nyquist plots obtained for the RC/IL films showed slight differences depending on the IL, but they differed significantly from the plot corresponding to the RC support also presented in Figure 7a for comparison reasons. On the other hand, the Z_{real} vs. frequency plot (Bode plot) drawn in Figure 7b shows clear differences among the samples in the interfacial region (electrode/film contribution, f < 100 Hz), which is an indication of film surface modification as it was already reported for nanoporous alumina modified structures [58]; moreover, a slight shift to lower frequency values for the maximum of the $-Z_{img}$ vs. frequency curves shown in Figure 7c for both RC/IL films with respect to that obtained for the RC-support can also be observed, which used to be attributed to a more compact film structure [46]. In this context, the Bode plot obtained for the IL AliquatCl was also included as an insert in Figure 7c, with the frequency value for the maximum of the IL curve of 500,000 Hz, much higher than that determined for the RC/AliquatCl film (~2800 Hz). In fact, modification in the electrical response of a dry polymeric (cellulose triacetate or CTA) membrane (or thin film) with the content of AliquatCl was already reported [57w], and the effect of the increase in the AliquatCl percentage on both the electrode/film interface and the bulk phase are presented as Supplementary Information (Figure S4).

The fit of the IS data points represented in Figure 7a to a parallel association of resistance (R_f) and a non-ideal capacitor (Q_f) for both RC/IL films (R_fQ_f equivalent circuit) allowed us to determine the electrical resistance and equivalent capacitance (C^{eq}) values [44], and from these results, the conductivity (σ_f) and dielectric constant (ε_f) of each RC/IL film were obtained, taking into account the following well-known expressions (valid for homogeneous conductors and plane–plate capacitors) [45]:

$$\sigma_f = \Delta x_f / S_f.R_r \quad (3)$$

$$\varepsilon_f = C_f.\Delta x_f / S_f.\varepsilon_o \quad (4)$$

where ε_o is the vacuum permittivity, while Δx_f and S_f represent the thickness and area of the films, respectively, and the values obtained for both parameters are: σ_f (RC/$BMIMPF_6$) = 4.4×10^{-6} $(\Omega.m)^{-1}$ and ε_f = 23.8, while σ_f (RC/AliquatCl) = 4.8×10^{-6} $(\Omega.m)^{-1}$ and ε_f = 28.1, causing a reduction of around 40–45% in the conductivity of the RC-support, but an increase of 10% for the RC/$BMIMPF_6$ film and 20% for the RC/AliquatCl one in the case of the dielectric constant, in agreement with that already reported [59]; consequently, the modification of the cellulosic support with both ILs increases its insulating character.

4. Conclusions

The incorporation of room-temperature ionic liquids (ILs) with different characteristics ($BMIMPF_6$ or AliquatCl) into a biocompatible regenerated cellulose (RC) film, by only 1 h immersion in the corresponding IL, permits the modification of the mechanical and electrical characteristics of the RC support, which were determined by tensile and impedance spectroscopy measurements. XPS resolved-angle measurements carried out for the RC/$BMIMPF_6$ and RC/AliquatCl films showed the presence of the ILs in the ~10 nm film top layer, indicating a higher coverage of the RC-support by the AliquatCl IL. The coverage with the ILs practically did not modify the transmission/reflexion of the RC-support, but increased its insulating behavior (conductivity reduction and dielectric constant increase); moreover, ILs incorporation favored the mechanical stability of the RC-support, increasing the Young modulus of both RC/ILs films (with differences depending on the IL) significantly. In this context, since ILs can be easily modified, it should be possible to obtain eco-friendly or biocompatible RC/IL composite materials with characteristics of interest for specific applications (biomedical and pharmaceutical applications) by a simple process (without chemical reactions). The effect of immersion time on the parameters studied is a point for further consideration.

Supplementary Materials: The following supporting information can be downloaded at https://www.mdpi.com/article/10.3390/app122010290/s1: Figure S1: Chemical formula of: (a) AliquatCl, (b) ILBMIMPF$_6$ IL and (c) regenerated cellulose; Figure S2: (a) Comparison of N 1*s* core level signal determined for a 40% CTA + 60% AliquaCl sample in dry (blue solid line) and hydrated (blue dashed dashed line) states. (b) Comparison of normalized N 1*s* core level signal for the RC/BMIMPF$_6$ film (red solid line) and BMIMPF$_6$ IL (red dashed line); Figure S3: Stain vs. stress curves measured with: (a) a dry RC film, (b) a wet RC film (after 72 h in distilled water); Figure S4: Impedance plots for two CTA/AliquatCl membranes with different AliquatCl content; Table S1: Atomic concentration percentages of the elements detected on the surfaces of the BMIMPF$_6$ and AliquatCl ILs and the RC-support film.

Author Contributions: J.B. designed and coordinated the experiments; M.d.V.M.d.Y. performed and analyzed the XPS measurements; A.L.C. carried out the optical characterization; impedance spectroscopy measurements and data analysis were performed by J.B. All authors have read and agreed to the published version of the manuscript.

Funding: This research received no external funding.

Data Availability Statement: The date can be found in Supplementary Materials.

Acknowledgments: To David Marrero (Applied Physics I Department, University of Málaga, Spain) for his support.

Conflicts of Interest: The authors declare no conflict of interest.

References

1. Singh, S.K.; Savoy, A.W. Ionic liquids synthesis and applications: An overview. *J. Mol. Liquids* **2020**, *297*, 112038. [CrossRef]
2. Welton, T. Room temperature ionic liquids. Solvent for synthesis and catalysis. *Chem. Rev.* **1999**, *99*, 2071. [CrossRef] [PubMed]
3. Abott, A.P.; McKenzie, K. Application of ionic liquids to the electrodeposition of metals. *Phys. Chem. Chem. Phys.* **2006**, *8*, 4265–4279. [CrossRef]
4. Matsumoto, H.; Sakaebe, H.; Tatsumi, K. Preparation of room temperature ionic liquids based on aliphatic onium cations and asymmetrc amide anions as a lithium battery electrode. *J. Power Sources* **2006**, *160*, 1308–1313. [CrossRef]
5. Paul, A.; Mandal, P.K.; Samanta, A. On the optical properties of the imidazolium ionic liquids. *Am. Chem. Soc.* **2005**, *109*, 9148–9153. [CrossRef] [PubMed]
6. Yuyama, K.; Masuda, G.; Yoshida, H.; Sato, T. Ionic liquids containing the tetrafluoroborate anion have the best performance and stability for electric double layer capacitor applications. *J. Power Sources* **2006**, *162*, 1401–1408. [CrossRef]
7. Armand, M.; Endres, F.; MacFarlane, D.R.; Ohno, H.; Scrosati, B. Ionic Liquids materials for the electrochemical changes of the future. *Nat. Mater.* **2009**, *8*, 621–629. [CrossRef] [PubMed]
8. Zhao, Y.; Bostrom, T. Application of Ionic Liquids in solar cells and batteries: A review. *Curr. Org. Chem.* **2015**, *19*, 556–566. [CrossRef]
9. Rojas, V.; Martínez, F.; Bernède, J.C.; Guenadez, L.C.; Efimov, A.; Lemmetyinen, H. Alkyl Thiophene Vinylene Electropolimerization in C_8mimPF$_6$, Potential Use in Solar Cells. *Mater. Sci. Appl.* **2017**, *8*, 405–417.
10. Piatti, E.; Guglielmero, L.; Tofani, G.; Mezzetta, A.; Guazzelli, L.; D'Andrea, F.; Roddaro, S.; Pomelli, C.S. Ionic liquids for electrochemical applications: Correlation between molecular structure and electrochemical stability window. *J. Mol. Liquids* **2022**, *364*, 120001. [CrossRef]
11. Tang, X.; Lv, S.; Jiang, K.; Zhou, G.; Liu, X. Recent development of ionic liquid-based electrolytes in lithium-ion batteries. *J. Power Sources* **2022**, *542*, 231792. [CrossRef]
12. Behera, K.; Pandey, S.; Kadyan, A.; Pandey, S. Ionic-liquid based optical and electrochemical carbon dioxide sensors. *Sensors* **2015**, *15*, 30487–30503. [CrossRef]
13. Neves, L.A.; Benavente, J.; Coelhoso, I.M.; Crespo, J.G. Design and characterization of Nafion membranes with incorporated ionic liquids cations. *J. Membr. Sci.* **2010**, *347*, 42–52. [CrossRef]
14. Mikkola, J.-P.; Virtanen, P.; Sjöholm, R. Aliquat 336®-a versátil and afforable catión source for an entirely new family of hydrophobic ioni liquids. *Green Chem.* **2006**, *8*, 250–255. [CrossRef]
15. Fontàs, C.; Vera, R.; Anticó, E.; Martínez de Yuso, M.V.; Rodríguez-Castellón, E.; Benavente, J. New Insights on the Effects of Water on Polymer Inclusion Membranes Containing Aliquat Derivatives as Carriers. *Membranes* **2022**, *12*, 192. [CrossRef]
16. Correia, D.M.; Fernandes, L.C.; Fernandes, M.M.; Hermenegildo, M.; Meira, R.M.; Ribeiro, C.; Ribeiro, S.; Reguera, J.; Lanceros-Méndez, S. Ionic Liquid-Based Materials for Biomedical Applications. *Nanomaterials* **2021**, *11*, 2401. [CrossRef]
17. Fortunato, R.; Branco, L.C.; Afonso, C.A.M.; Benavente, J.; Crespo, J. Electrical impedance spectroscopy characterization of supported ionic liquid membranes. *J. Membr. Sci.* **2006**, *270*, 42–49. [CrossRef]
18. Figueroa, J.D.; Fout, T.; Plasynki, S.; McIlvried, H.; Srivastava, R.D. Advances in CO_2 capture technology-The U.S. Department of energy´s carbon sequestration program. *Int. J. Greenh. Gas Control* **2008**, *2*, 9–20. [CrossRef]

19. Salar-García, M.J.; Ortíz-Martínez, V.M.; de los Ríos, A.P.; Hernádez-Fernández, F.J. A method based on impedance spectroscopy for predicting the behaviour of novel ionic liquid-polymeric inclusion membranes in microbial cells. *Energy* **2015**, *89*, 648–654. [CrossRef]
20. Gao, H.; Bai, L.; Han, J.; Yang, B.; Zhang, S.; Zhang, X. Functionalized ionic liquid membranes for CO_2 separation. *Chem. Commun.* **2018**, *54*, 12671–12685. [CrossRef]
21. Neves, L.A.; Crespo, J.G.; Coelhoso, I.M. Gas Permeation Studies in Supported Ionic Liquid Membranes. *J. Membr. Sci.* **2010**, *357*, 160–170. [CrossRef]
22. Schmidt, C.; Glück, T.; Schmidt-Naake, G. Modification of Nafion Membranes by Impregnation with Ionic Liquids. *Chem. Eng. Technol.* **2008**, *31*, 13–22. [CrossRef]
23. Neves, L.A.; Coelhoso, I.M.; Crespo, J.G. Methanol and gas crossover through modified nafion membranes by incorporation of ionic liquids cations. *J. Membr. Sci.* **2010**, *357*, 160–170. [CrossRef]
24. Martínez de Yuso, M.V.; Neves, L.A.; Coelhoso, I.M.; Crespo, J.G.; Benavente, J.; Rodríguez-Castellón, E. A Study of Chemical Modifications of a Nafion Membrane by Incorporation of Different Room Temperature Ionic Liquids. *Fuel Cells* **2012**, *12*, 606–612. [CrossRef]
25. Martínez de Yuso, M.V.; Arango-Díaz, A.; Bijani, S.; Romero, V.; Benavente, J.; Rodríguez-Castellón, E. Chemical Surface, Thermal and Electrical Characterization of Nafion Membranes Doped with IL-Cations. *Appl. Sci.* **2014**, *4*, 195–206. [CrossRef]
26. Kumar, R.; Pandey, A.K.; Sharma, M.K.; Panicker, L.V.; Sodaye, S.; Suresh, G.; Ramagiri, S.V.; Bellare, J.R.; Goswami, A. Diffusional transport of ions in plasticized anion-exchange membranes. *J. Phys. Chem. B* **2011**, *115*, 5856–5867. [CrossRef]
27. Matsumoto, M.; Murakami, Y.; Minamidate, Y.; Kondo, K. Separation of lactic acid through polymer inclusión membranes containing ionic liquids. *Sep. Sci. Technol.* **2012**, *47*, 354–359. [CrossRef]
28. Vázquez, M.I.; Romero, V.; Fontàs, C.; Anticó, E.; Benavente, J. Polymer inclusion membranes (PIMs) with the ionic liquid (IL) Aliquat 336 as extractant: Effect of base polymer nature and IL concentration on their physical-chemical and elastic characteristics. *J. Membr. Sci.* **2014**, *445*, 312–319. [CrossRef]
29. Gherasian, C.-V.; Borceanu, G.; Olariu, R.-I.; Arnese, C. A novel polymer inclusión membrane applied in chromium (VI) separation from aqueous solutions. *J. Hazard. Mater.* **2011**, *197*, 244–253. [CrossRef] [PubMed]
30. Benavente, J.; Romero, V.; Vázquez, M.I.; Anticó, E.; Fontàs, C. Electrochemical Characterization of a Polymer Inclusion Membrane Made of Cellulose Triacetate and Aliquat 336 and Its Application to Sulfonamides Separation. *Separations* **2018**, *5*, 5. [CrossRef]
31. Soheilmoghaddam, M.; Sharifzadeh, G.; Pour, R.H.; Wahit, M.U.; Whye, W.T.; Lee, X.Y. Regenerated cellulose/β-cyclodextrin scaffold prepared using ionic liquid. *Mater. Lett.* **2014**, *135*, 210–213. [CrossRef]
32. Benavente, J.; Vázquez, M.I.; Hierrezuelo, J.; Rico, R.; López-Romero, J.M.; López-Ramirez, M.R. Modification of a Regenerated Cellulose Membrane with Lipid Nanoparticles and Layers. Nanoparticle Preparation, Morphological and Physicochemical Characterization of Nanoparticles and Modified Membranes. *J. Membr. Sci.* **2010**, *355*, 45–52. [CrossRef]
33. Zeng, J.; Yan, L. Metal-free transparent luminescent cellulose films. *Cellulose* **2015**, *22*, 729–736. [CrossRef]
34. Vázquez, M.I.; Algarra, M.; Benavente, J. Modification of regenerated cellulose membrane modified with thiol dendrimer. *Carbohydr. Polym.* **2015**, *131*, 273–279. [CrossRef]
35. Cuevas, A.; Campos, B.B.; Romero, R.; Algarra, M.; Vázquez, M.I.; Benavente, J. Eco-friendly modification of regenerated cellulose based film by silicon, carbon, and N-doped carbon quantum dots. *Carbohydr. Polym.* **2019**, *206*, 238–244. [CrossRef] [PubMed]
36. Benavente, J.; García, M.E.; Urbano, N.; López-Romero, J.M.; Contreras-Cáceres, R.C.; Casado-Rodríguez, M.A.; Moscoso, A.; Hierrezuelo, J. Inclusion of silver nanoparticles for improving regenerated cellulose membrane performance and reduction of biofouling. *Int. J. Biol. Macrom.* **2017**, *103*, 758–763. [CrossRef] [PubMed]
37. You, Y.; Zhang, H.; Liu, Y.; Lei, B. Transparent sunlight conversion film based on carboxymethyl cellulose and carbon dots. *Carbohydr. Polym.* **2016**, *151*, 245–250. [CrossRef]
38. Miao Zou, M.; Chen, Y.; Chang, L.; Cheng, X.; Gao, L.; Guo, W.; Ren, Y.; Shupin, L.; Tang, Q. Toward 90 μm Superthin Transparent Wood Film Impregnated with Quantum Dots for Color-Converting Materials. *ACS Sustain. Chem. Eng.* **2022**, *10*, 2097–2106.
39. Litaiem, Y.; Dhahbi, M. Physicochemical properties of an hydrophobic ionic liquid (Aliquat 336) in a polar protic solvent (formamide) at different temperatures. *J. Disp. Sci. Technol.* **2015**, *36*, 641–651. [CrossRef]
40. Benavente, J.; Rodríguez-Castellón, E. Application of electrochemical impedance spectroscopy (EIS) and X-ray photoelectron spectroscopy (XPS) to the characterization of RTILs for electrochemical applications. In *Ionic Liquids: Applications and Perspectives*; Kokorin, A., Ed.; INTECH: Rijeka, Croatia, 2011; Chapter 27; pp. 607–626.
41. Lockett, V.; Sedev, R.; Bassell, C.; Ralston, J. Angle-resolved X-ray photoelectron spectroscopy of the surface of imidazolium ionic liquids. *Phys. Chem. Chem. Phys.* **2008**, *10*, 1330–1335. [CrossRef]
42. Lukas, J.; Jezek, B. Inelastic mean free paths of photoelectrons from polymer surfaces determined by the XPS method. *Collect. Czechoslov. Chem. Commun.* **1983**, *48*, 2909–2913. [CrossRef]
43. Multitechnique ESCA. *Software Reference Manual for the PC-ACCESS Software*; Version 6.0.; Physical Electronics: Minneapolis, MI, USA, 1995.
44. Moulder, J.F.; Stickle, W.F.; Sobol, P.E.; Bomben, K.D. *Handbook of X-Ray Photoelectron Spectroscopy*; Chastain., J., Ed.; Perkin-Elmer Corporation: Minneapolis, MI, USA, 1992.
45. Macdonald, J.R.; Johnson, W.B. Fundamentals of Impedance Spectroscopy. In *Impedance Spectroscopy: Theory, Experiment, and Applications*, 3rd ed.; Barsoukov, E., Ed.; Wiley Online Library: Hoboken, NJ, USA, 2018. [CrossRef]

46. Benavente, J. Use of Impedance Spectroscopy for characterization of modified membranes. In *Membrane Modification: Technology and Applications. Hilal, N., Kayet, M., Wright, C.J., Eds.*; CRC Press: Boca Raton, FL, USA, 2012; ISBN 9781439866368.
47. Brigg, D.; Seah, M.P. *Practical Surface Analysis: Auger and X-Ray Photoelectron Spectroscopy*, 2nd ed.; John Wiley & Sons: Chichester, UK, 1995; Volume 1.
48. Simon, M.; Fulchiron, R.; Gouanvé, F. Water Sorption and Mechanical Properties of Cellulosic Derivative Fibers. *Polymers* **2022**, *14*, 2836. [CrossRef] [PubMed]
49. Vázquez, M.I.; De Lara, R.; Benavente, J. Transport and elastic parameters of regenerated cellulose membranes: Temperature effect. *Desalination* **2009**, *245*, 579–586. [CrossRef]
50. Saedi, S.; Garcia, C.V.; Kim, J.T.; Shin, G.H. Physical and chemical modifications of cellulose fibers for food packaging applications. *Cellulose* **2021**, *28*, 8877–8897. [CrossRef]
51. Krishnan, R.; Pandiaraj, S.; Muthusamy, S.; Panchal, H.; Alsoufi, M.S.; Ibrahim, A.M.M.; Elsheikh, A. Biodegradable magnesium metal matrix composites for biomedical implants: Synthesis, mechanical performance, and corrosion behavior—A review. *J. Mater. Res. Technol.* **2022**, *20*, 650–670.
52. Ramos, J.D.; Milano, C.; Romero, V.; Escalera, S.; Alba, M.C.; Vázquez, M.I.; Benavente, J. Water effect on physical-chemical and elastic parameters for a dense cellulose regenerated membrane. Transport of different aqueous electrolyte solutions. *J. Membr. Sci.* **2010**, *352*, 153–159. [CrossRef]
53. Reddy, K.O.; Maheswari, C.U.; Dhlamini, M.S.; Mothudi, B.M.; Zhang, J.; Zhang, J.; Nagarajan, R.; Rajulu, A.V. Preparation and characterization of regenerated cellulose films using borassus fruit fibers and an ionic liquid. *Carbohydr. Polym.* **2017**, *160*, 203–211. [CrossRef]
54. Cuevas, A.L.; Martínez de Yuso, M.V.; Vega, V.; González, A.S.; Prida, V.M.; Benavente, J. Influence of ALD coating layers on optical properties of nanoporous alumina-based structures. *Coatings* **2019**, *9*, 43. [CrossRef]
55. Gelde, L.; Cuevas, A.L.; Benavente, J. Influence of Pore-Size/Porosity on Ion Transport and Static BSA Fouling for TiO_2-Covered Nanoporous Alumina Membranes. *Appl. Sci.* **2021**, *11*, 5687. [CrossRef]
56. Algarra, M.; Cuevas, A.L.; Valle Martínez de Yuso, M.V.; Romero, R.; Alonso, B.; Casado, C.M.; Benavente, J. Optical and Physicochemical Characterizations of a Cellulosic/CdSe-QDs@S-DAB_5. *Nanomaterials* **2022**, *12*, 484. [CrossRef] [PubMed]
57. Vera, R.; Gelde, L.; Anticó, E.; Martínez de Yuso, M.V.; Benavente, J.; Fontàs, C. Tuning physicochemical, electrochemical and transport characteristics of polymer inclusion membrane by varying the counter-anion of the ionic liquid Aliquat 336. *J. Membr. Sci.* **2017**, *529*, 87–94. [CrossRef]
58. González, A.S.; Vega, V.; Cuevas, A.L.; Martínez de Yuso, M.V.; Prida, V.M.; Benavente, J. Surface Modification of Nanoporous Anodic Alumina during Self-Catalytic Atomic Layer Deposition of Silicon Dioxide from (3-Aminopropyl)Triethoxysilane. *Materials* **2021**, *14*, 5052. [CrossRef] [PubMed]
59. Shi, L.; Zhang, C.; Du, Y.; Zhu, H.; Zhang, Q.; Zhu, S. Improving Dielectric Constant of Polymers through Liquid Electrolyte Inclusion. *Adv. Funct. Mater.* **2021**, *31*, 2007863. [CrossRef]